MATHEMATICAL MODELING AND COMPUTING, Vol. 10, No. 1, pp. 10–29 (2023)

Homogenization of subwavelength free stratified edge of viscoelastic media including finite size effect

Belemou R.[1], Sbitti A.[2], Marigo J.-J.[3], Tsouli A.[4]

[1] *University Hassan II, Ens, El Jadida Km 9 Str, Ghandi, 50069, Casablanca, Maroc*
[2] *University Mohammed V, Ensam, Nations Unies Str, Agdal, 8007.N.U, Rabat, Maroc*
[3] *Solid Mechanics Laboratory, Ecole Polytechnique, 91128, Palaiseau, France*
[4] *University Hassan II, Ensam, 150 Nile Str, Sidi Othman, 20670, Casablanca, Maroc*

(Received 4 August 2022; Accepted 9 November 2022)

This paper proposes the homogenization for a stratified viscoelastic media with free edge. We consider the effect of two-dimensional periodically stratified slab over a semi-infinite viscoelastic ground on the propagation of shear waves hitting the interface. Within the harmonic regime, the second order homogenization and matched-asymptotic expansions method is employed to derive an equivalent anisotropic slab associated with effective boundary and jump conditions for the displacement and the normal stress across an interface. The reflection coefficients and the displacement fields are obtained in closed forms and their validity is inspected by comparison with direct numerics in the case of layers associated with Neumann boundary conditions.

Keywords: *homogenization; matched asymptotic expansion; reflection of waves; viscoelastic; stratified media; effective jump conditions.*

2010 MSC: 74Q05 **DOI:** 10.23939/mmc2023.01.010

1. Introduction

There is increasing demand for methods to estimate effective parameters of viscoelastic composites, e.g. vibration and noise control in structures. An effective model associated with shear waves scattering by a periodically stratified slab in viscoelastic with free edge and satisfying $\varepsilon = K_R h \ll 1$, where K_R being the real part of the complex shear wavenumber K^* and h the periodicity of the structure, is studied. It is easy to understand that in these cases, the numerical calculation of the solution would become prohibitive on a small scale, since the mesh used must accurately resolve the rapid variations. In order to overcome this difficulty, we will derive so-called effective boundary and jump conditions of the displacement and normal stress through an equivalent homogeneous anisotropic slab. The numerical discretization of the homogenized problem should be much less expensive than the exact mesh, since the mesh used does not have to be constrained by the small scale. There are several works that deal with the same kind of problem, for example, if the whole (or a large part of) the propagating medium has a micro-structuring whose smallest scale is below the wavelength, it is possible to simplify the model by using classical homogenization which derives an equivalent homogenized problem, see for example [1, 2]. In other situations, if only a small or thin region contains micro-structuring; they are originally developed in the context of solid mechanics [3–5], the homogenization of interfaces has been studied on some problems, especially in electromagnetism [6, 7], and acoustics [3–8]. In this article, we used asymptotic analysis and the same homogenization approach that was applied in the case of shear wave scattering by a periodically stratified slab in elasticity [9]. We noticed that in the case of viscoelastic media, the wave equation of the real problem takes the same form, except that in our case, the coefficients of physical parameters entering the equation are complex. That is why the homogenization procedure is the same and even the form of the homogenized wave equations obtained at different orders. Evenly, we establish that the second order homogenization reveals interface parameters, which enter into the jump conditions at the boundaries of the equivalent free edge slab (Figure 1). It is also showed that scattering parameters of effective model accurately describe those of the actual structure and in general the homogenized solution at the second order is even more significant than that at the first order. The paper is organized as follows. In Section 2, we summarize the result of the asymptotic analysis in the case of two viscoelastic media of a free stratified edge and an infinite substrate with a common interface boundary in welded contact, whose main steps of derivation is given in the Appendix 4. The resulting system (10) represents the homogenized problem associated with effective boundary and jump conditions of the displacement and of the normal stress across an equivalent homogeneous anisotropic slab. In Section 3, the accuracy of the effective model is inspected by comparison with direct numerics based on multimodal method [10] for a shear wave incident. The reflection coefficients as a function of the frequency $K_R h$ and thickness of the stratified structure e/h, and as a function of the reciprocal quality factor Q^{-1} are exemplified and the agreement between the actual and effective problems is discussed. We finish the study in Section 4 with concluding remarks and perspectives.

2. The actual problem and the effective problem

Below we summarize the main results of the analysis developed in the Appendix 4 and which provides the so-called (Effective problem) where the stratified medium is replaced by an equivalent anisotropic slab associated with the effective boundary at $X_1 = 0$ and the jump conditions for the displacement and the normal stress across an interface at $X_1 = e$ (Figure 1).

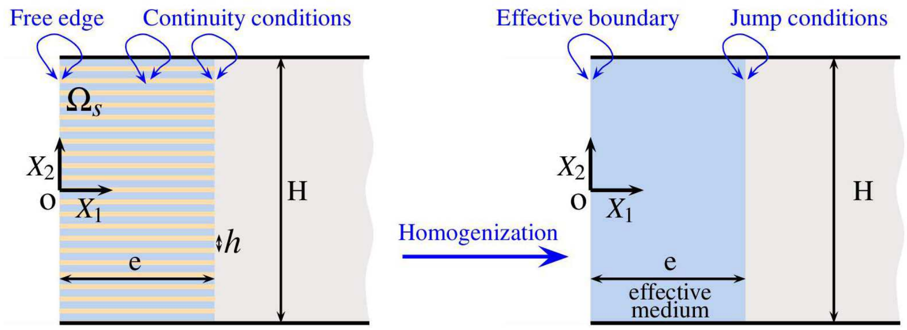

Fig. 1. On the left, the actual configuration of an viscoelastic body (in grey) with a viscoelastic stratified medium Ω_s. On the right, the homogenized configuration where the stratified medium is replaced by an equivalent homogeneous anisotropic slab, which associated with effective boundary and jump conditions apply at the boundaries of slab.

2.1. The physical problem

We consider the shear wave scattering by a welded boundary between a free stratified edge and an infinite isotropic viscoelastic substrate. The scalar displacement field $U(\mathbf{X})$ written in the harmonic regime wave (Figure 1), with $\mathbf{X} \in \Omega$ the spatial coordinates and $\Omega = \{(X_1, X_2) \in (0, +\infty) \times (-H/2, H/2)\}$,

$$\operatorname{div}(M \boldsymbol{\nabla} U) + \rho\,\omega^2 U = 0 \tag{1}$$

with M and ρ being the complex shear modulus and the mass density respectively, and ω is the frequency. Equation (1) can be written using the non-dimensional parameters,

$$\alpha^*(\mathbf{X}) \equiv \frac{M(\mathbf{X}, \omega)}{M_m} \quad \text{and} \quad \beta(\mathbf{X}) \equiv \frac{\rho(\mathbf{X})}{\rho_m}$$

with M_m the complex shear modulus and ρ_m the mass density of the substrate beside the stratified medium occupying the region $\Omega_s = \{(X_1, X_2) \in (0, e) \times (-H/2, H/2)\}$; with $K^* = \omega\sqrt{\rho_m/M_m}$ the complex wave number in the substrate Ω/Ω_s, we get

$$\operatorname{div}(\alpha^* \nabla U) + \beta K^{*2} U = 0. \tag{2}$$

What allows us to write the Helmholtz equation in the substrate as follows:

$$\Delta U + K^{*2} U = 0.$$

In the harmonic regime, we consider viscoelastic waves with a minimum wavelength $2\pi/K_R$ larger than the typical periodicity of the stratified structure h (K_R being the real part of the complex shear wavenumber K^*), such that

$$\varepsilon = K_R h \ll 1.$$

To be consistent, we shall work in dimensionless coordinate $\mathbf{x} = (x_1, x_2)$ and on a problem simplified with respect to that in (Figure 1) in the sense that we can determine the effective boundary conditions at $x_1 = 0^+$ and the jump conditions at $x_1 = e$.

2.1.1. Stratified structure ending with Neumann boundary condition

To determine the effective boundary conditions at $x_1 = 0^+$ with ($x_1 = K_R X_1$, $x_2 = K_R X_2$), we consider the first actual problem for $\mathbf{x} = (x_1, x_2) \in (0, +\infty,) \times (-K_R H/2, K_R H/2)$ and $\sigma_1^\varepsilon(0^+, x_2) = 0$ (Figure 2), where the infinite stratified medium occupies the half space $x_1 > 0$ with Neumann boundary condition at $x_1 = 0^+$. We denote

$$a^{*\varepsilon}(\mathbf{x}) \equiv \alpha^*(\mathbf{X}), \quad b^{*\varepsilon}(\mathbf{x}) \equiv \beta(\mathbf{X}) \left(\frac{K^*}{K_R}\right)^2; \quad u^\varepsilon(\mathbf{x}) \equiv U(\mathbf{X}), \quad \sigma^\varepsilon(\mathbf{x}) \equiv {K_R}^{-1} \alpha^*(\mathbf{X}) \nabla U(\mathbf{X}),$$

where the functions a^* and b^* are 1-periodic and complex, such that

$$a^{*\varepsilon}(\mathbf{x}) = a^*\left(\frac{x_2}{\varepsilon}\right) \quad \text{and} \quad b^{*\varepsilon}(\mathbf{x}) = b^*\left(\frac{x_2}{\varepsilon}\right). \tag{3}$$

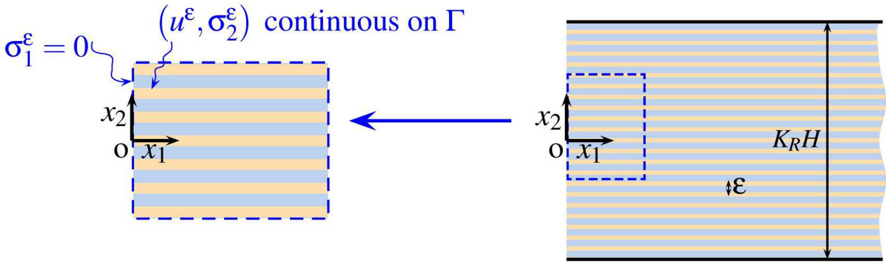

Fig. 2. Stratified medium occupying the region $x_1 > 0$ and the substrate occupying the region $x_1 > 0$ with a free edge at $x_1 = 0$. The usual continuity conditions apply at the boundaries Γ between the layers $(u^\varepsilon, \sigma_2^\varepsilon)$ and Neumann boundary condition $\sigma_1^\varepsilon = 0$ applies at $x_1 = 0$.

Also, we indicated explicitly the dependence of $(u^\varepsilon, \sigma^\varepsilon)$ on ε being the periodicity of the stratified medium in non dimensional form. Now (2) reads

$$\begin{cases} \operatorname{div} \sigma^\varepsilon(\mathbf{x}) + b^{*\varepsilon}(\mathbf{x}) u^\varepsilon(\mathbf{x}) = 0, \quad x_1 > 0, \\ \sigma^\varepsilon(\mathbf{x}) = a^{*\varepsilon}(\mathbf{x}) \nabla u^\varepsilon(\mathbf{x}), \\ \sigma_1^\varepsilon\left(0^+, x_2\right) = 0, \\ u^\varepsilon \text{ and } \sigma^\varepsilon \cdot \mathbf{n} \text{ continuous on } \Gamma \end{cases} \tag{4}$$

with $\mathbf{x} \in (0, +\infty) \times (-K_R H/2, K_R H/2)$ and Γ the boundaries between two layers within the stratified medium (Figure 2); finally, appropriate boundary conditions at $x_1 \to +\infty$ and $x_2 = \pm K_R H/2$, often referred to as radiation conditions, apply once the wave source has been defined. For the time being, we do not need to specify their form.

2.1.2. Welded boundary between an infinite layers and substrate

To derive the jump conditions between the stratified medium and substrate, we focus on a region near the boundary of the stratified medium at $X_1 = e$; and to do that, we assume that the stratified medium occupies the region $x_1 < 0$ with ($x_1 = K_R(X_1 - e)$, $x_2 = K_R X_2$). Doing so, we assume implicitly that the wave passing through the stratified slab in the configuration of (Figure 3) feels the boundaries and the bulk of the stratified medium. This means that the slab is thick enough, and thick means that the evanescent fields at both boundaries of the slab do not interact.

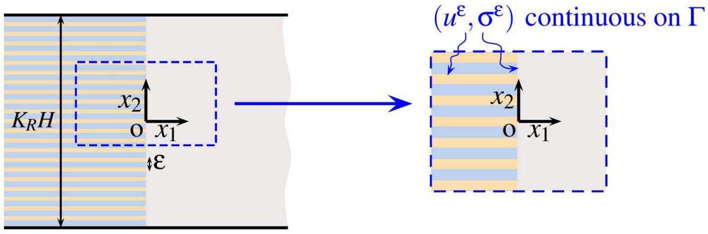

Fig. 3. Single interface between the stratified medium occupying the region $x_1 < 0$ and the substrate occupying the region $x_1 > 0$. The usual continuity conditions apply at the boundaries Γ between the layers $(u^\varepsilon, \sigma_2^\varepsilon)$ and at the boundaries between the layers and the substrate $(u^\varepsilon, \sigma_1^\varepsilon)$ at $x_1 = 0$.

The second actual problem for $\mathbf{x} = (x_1, x_2) \in \mathbb{R} \times (-K_R H/2, K_R H/2)$, reads as

$$\begin{cases} \operatorname{div} \sigma^\varepsilon(\mathbf{x}) + b^{*\varepsilon}(\mathbf{x}) u^\varepsilon(\mathbf{x}) = 0, & |x_1| > 0, \\ \sigma^\varepsilon(\mathbf{x}) = a^{*\varepsilon}(\mathbf{x}) \nabla u^\varepsilon(\mathbf{x}), & \\ u^\varepsilon \text{ and } \sigma^\varepsilon \cdot \mathbf{n} \text{ continuous}, & \Gamma, x_1 = 0 \end{cases} \tag{5}$$

where in this case, the functions a^* and b^* are 1-periodic and piecewise complex constant, such that

$$a^{*\varepsilon}(\mathbf{x}) = \begin{cases} 1, & x_1 > 0, \\ a^*\left(\frac{x_2}{\varepsilon}\right), & x_1 < 0, \end{cases} \qquad b^{*\varepsilon}(\mathbf{x}) = \begin{cases} (\frac{K^*}{K_R})^2, & x_1 > 0, \\ b^*\left(\frac{x_2}{\varepsilon}\right), & x_1 < 0. \end{cases} \tag{6}$$

The boundary conditions at $|x_1| \to +\infty$ and $x_2 = \pm K_R H/2$ are considered the same of (4).

2.2. The effective problem

Firstly, we shall determine the homogenized problems of the first and second actual problems (4)–(5). The homogenized problem of stratified structure ending with Neumann boundary condition (4), is done by defining the fields (u^h, σ^h) satisfying the following problem:

$$\begin{cases} \operatorname{div} \boldsymbol{\sigma}^h + \langle b^* \rangle u^h = 0, \quad \boldsymbol{\sigma}^h = \begin{pmatrix} \langle a^* \rangle & 0 \\ 0 & \langle 1/a^* \rangle^{-1} \end{pmatrix} \nabla u^h, \quad x_1 > 0, \\ {\sigma_1}^h\left(0^+, x_2\right) = 0. \end{cases} \tag{7}$$

and the average over $y_2 \in Y$ for any function f, is defined by

$$\langle f \rangle(\mathbf{x}) \equiv \int_Y \mathrm{d}y_2\, f(\mathbf{x}, y_2).$$

The second homogenized problem of a welded boundary between an infinite layers and substrate (5), reads as

$$\begin{cases} \operatorname{div} \sigma^h + \langle b^* \rangle u^h = 0, \quad \sigma^h = \begin{pmatrix} \langle a^* \rangle & 0 \\ 0 & \langle 1/a^* \rangle^{-1} \end{pmatrix} \nabla u^h, & x_1 < 0, \\ \operatorname{div} \sigma^h + \left(\dfrac{K^*}{K_R}\right)^2 u^h = 0, \quad \sigma^h = \nabla u^h, & x_1 > 0, \\ [\![u^h]\!] = \dfrac{\varepsilon \mathcal{B}}{2}\left[\sigma_1^h\left(0^-, x_2\right) + \sigma_1^h(0^+, x_2)\right], & \\ [\![\sigma_1^h]\!] = -\dfrac{\varepsilon \mathcal{C}}{2}\left[\dfrac{\partial^2 u^h}{\partial x_2^2}(0^-, x_2) + \dfrac{\partial^2 u^h}{\partial x_2^2}(0^+, x_2)\right], & \end{cases} \tag{8}$$

where $(\mathcal{B}, \mathcal{C})$ are the interface parameters and we defined

$$[\![f]\!] \equiv f\left(0^+, x_2, \tau\right) - f\left(0^-, x_2, \tau\right) \tag{9}$$

for any outer terms f being discontinuous across an equivalent interface at $x_1 = 0$, with $(f^-; f^+)$ its values on both sides.

Finally, from (7)–(8) and coming back to the real space with a welded boundary is considered at $X_1 = e$, in the $\mathbf{X} = \mathbf{x}/K_R$ coordinate and with $U^h(\mathbf{X}) = u^h(\mathbf{x})$, $\Sigma^h(\mathbf{X}) = K_R\sigma^h(\mathbf{x})$, we get an effective problem

$$\begin{cases} \operatorname{div}\Sigma^h + \langle b^*\rangle {K_R}^2 U^h = 0, \quad \Sigma^h = \begin{pmatrix} \langle a^*\rangle & 0 \\ 0 & \langle 1/a^*\rangle^{-1} \end{pmatrix} \nabla U^h, \quad 0 < X_1 < e, \\ \operatorname{div}\Sigma^h + {K^*}^2 U^h = 0, \quad \Sigma^h = \nabla U^h, \qquad X_1 > e, \\ [\![U^h]\!] = \dfrac{hB}{2}\left[\Sigma_1^h(e^-, X_2) + \Sigma_1^h(e^+, X_2)\right], \\ [\![\Sigma_1^h]\!] = -\dfrac{hC}{2}\left[\dfrac{\partial^2 U^h}{\partial X_2^2}(e^-, X_2) + \dfrac{\partial^2 U^h}{\partial X_2^2}(e^+, X_2)\right], \\ {\Sigma_1}^h(0^+, x_2) = 0. \end{cases} \tag{10}$$

3. Numerical validation of the effective problem

In this section, we address the error of the homogenized solution when compared to the solution of the actual problem, we shall consider the particular scattering problem of the reflection of rectangular voids, free of stresses (with Neumann conditions on their boundaries), periodically spaced in a homogeneous matrix being composed of the same linear viscoelastic material as the substrate. In acoustics, this corresponds to an array of sound hard material in a fluid; in electromagnetism to a (perfect conducting) metallic array in a dielectric or in the air.

3.1. Solutions of the physical problem

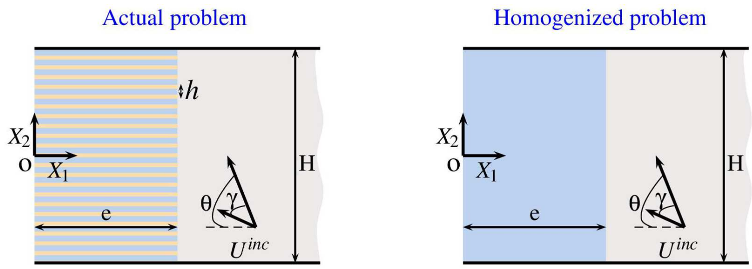

Fig. 4. Left: Actual problem of the scattering of a plane wave at oblique incidence θ an array of rectangular voids, with degree of inhomogeneity γ. Right: The homogenized problem involves a slab of same thickness e filled with a homogeneous anisotropic material, which associated with jump conditions apply at $X_1 = \pm e$.

We solve numerically the actual problem of an incident shear wave as a Type-II S wave [11], which coming from $X_1 > e$ and hitting the array at oblique incidence θ with degree of inhomogeneity γ (Figure 4). This is done using a multimodal method, which is detailed in [12]. We shall work in the harmonic regime, the complex fields (and we shall consider the displacement field $U(\mathbf{X})$) have a time dependence in $e^{-\mathrm{i}\omega t}$ and it will be omitted in the following. The incident wave is considered as below

$$U^{\mathrm{inc}}(\mathbf{X}) = \mathrm{e}^{-\mathrm{i}\omega t}\mathrm{e}^{i\boldsymbol{K}\cdot\boldsymbol{r}} = \mathrm{e}^{-\mathrm{i}\omega t}\mathrm{e}^{-\boldsymbol{A}\cdot\boldsymbol{r}}\mathrm{e}^{i\boldsymbol{P}\cdot\boldsymbol{r}}, \tag{11}$$

where $\boldsymbol{r} = (X_1, X_2)$ is the position vector, and $\boldsymbol{K}$ the complex wave vector is given by

$$\boldsymbol{K} = \boldsymbol{P} + \mathrm{i}\boldsymbol{A} = K_S\hat{x_1} + K_{\mathrm{inc}}\hat{x_2}$$

and the corresponding propagation and attenuation vectors, are given by

$$\boldsymbol{P} = |\boldsymbol{P}|\cos(\theta)\,\hat{x_2} + |\boldsymbol{P}|\sin(\theta)\,\hat{x_2} = \mathrm{Re}\,[K_S]\,\hat{x_1} + \mathrm{Re}\,[K_{\mathrm{inc}}]\,\hat{x_2},$$
$$\boldsymbol{A} = |\boldsymbol{A}|\cos(\theta-\gamma)\,\hat{x_1} + |\boldsymbol{A}|\sin(\theta-\gamma)\,\hat{x_2} = \mathrm{Im}\,[K_S]\,\hat{x_1} + \mathrm{Im}\,[K_{\mathrm{inc}}]\,\hat{x_2},$$

with $(\hat{x_1}, \hat{x_2})$ are orthogonal real unit vectors for a Cartesian coordinate system, K_{inc} the complex wave number for the assumed general SII wave, and $K_S = \sqrt{{K^*}^2 - {K_{\mathrm{inc}}}^2}$, where "$\sqrt{\ }$" is understood to indicate the principal value of the square root of a complex number $z = z_R + \mathrm{i}\,z_I$ defined in terms of the positive square root of real numbers by

$$\sqrt{z} = \sqrt{\frac{|z| + z_R}{2}} + \mathrm{i}\,\mathrm{sign}\,[z_I] \sqrt{\frac{|z| - z_R}{2}}$$

with

$$\mathrm{sign}\,[z_I] \equiv \begin{cases} 1 & \text{if} \quad z_I \geqslant 0, \\ -1 & \text{if} \quad z_I < 0. \end{cases}$$

Hence, the complex wave numbers K_{inc} and K_S reads

$$K_{\mathrm{inc}} = |\boldsymbol{P}| \sin(\theta) + \mathrm{i}\, |\boldsymbol{A}| \sin(\theta - \gamma),$$
$$K_S = |\boldsymbol{P}| \cos(\theta) + \mathrm{i}\, |\boldsymbol{A}| \cos(\theta - \gamma),$$

where the magnitudes of the propagation and attenuation are specified in terms of the given material parameters, the complex wave number K^* or wave speed ($v_m = \omega/K_R$) and the reciprocal quality factors (${Q_m}^{-1} = M_{mI}/M_{mR}$), and the given degree of inhomogeneity γ [11].

The reference numerical solution U^{num} is sought in the substrate where the Helmholtz equation applies and Neumann boundary conditions apply at each free boundary of the viscoelastic body. The problem actual is set in Ω being the region occupied by the substrate and we denote Γ the boundary of the viscoelastic body were Neumann boundary condition applies, the problem reads

$$\begin{cases} \Delta U + {K^*}^2 U = 0, & \text{in } \Omega, \\ \boldsymbol{\Sigma} \cdot \mathbf{n} = 0, & \text{on } \Gamma, \\ \lim\limits_{X_1 \to +\infty} \left[\dfrac{\partial}{\partial X_1} \left(U - U^{\mathrm{inc}} \right) - \mathrm{i} K_S \left(U - U^{\mathrm{inc}} \right) \right] = 0, & \\ U\left(X_1, \dfrac{H}{2} \right) = e^{\mathrm{i} K_{\mathrm{inc}}} U \left(X_1, -\dfrac{H}{2} \right), & X_1 \in \mathbb{R}^+, \\ \dfrac{\partial U}{\partial X_2} \left(X_1, \dfrac{H}{2} \right) = e^{\mathrm{i} K_{\mathrm{inc}}} \dfrac{\partial U}{\partial X_2} \left(X_1, -\dfrac{H}{2} \right), & X_1 \in \mathbb{R}^+, \end{cases} \tag{12}$$

where the scattered waves $(U - U^{\mathrm{inc}})$ at $X_1 \to +\infty$ satisfy the radiation condition [13], and are considered in the low frequency regime [14]. The last condition represents the pseudo-periodicity [15], which applies in the case where $H = nh$ with n an integer, for the incident wave and for the total field.

3.2. Solutions of the effective problem

We shall inspect the accuracy of the homogenization at the first and the second order, to do so, we treat tow particular problems of scattering by an array of rectangular voids. Such that in the first case the free stratified edge is considered elastic and the substrate a viscoelastic media. In the second case, we consider that the free stratified edge and substrate are the same viscoelastic media.

3.2.1. The case of welded viscoelastic stratified edge with elastic substrate

The homogenized problems can be solved exactly in the limiting case of voids with $a = 0 = b$ (leading to the Neumann boundary condition at the boundary with any other material). Hereafter, we consider in this case that $a^* = 1$, $b^* = 1$ in the elastic substrate with reciprocal quality factor $Q_m^{-1} = 0$, and φ the filling fraction of the viscoelastic media in the stratified edge with reciprocal quality factor $Q_{in}^{-1} = 0.1$, the bulk parameters in the equivalent medium becomes $\langle a^* \rangle = \xi\varphi$ with ($\xi = \frac{M_i}{M_m}$); $\langle b^* \rangle = (\frac{\rho_i}{\rho_m})(\frac{K^*}{K_R})^2 \varphi$ and $\langle 1/a^* \rangle^{-1} = 0$, whence the homogenized wave equation (30) reads

$$\mathrm{div}\, \boldsymbol{\Sigma}^{\boldsymbol{h}} + \varphi {K_i^*}^2 U^h = 0, \quad \boldsymbol{\Sigma}^{\boldsymbol{h}} = \begin{pmatrix} \xi\varphi & 0 \\ 0 & 0 \end{pmatrix} \boldsymbol{\nabla} U^h$$

with M_i the complex shear modulus and ρ_i the mass density of the stratified edge occupying the region $\Omega_s = \{(X_1, X_2) \in (0, e) \times (-H/2, H/2)\}$; with $K_i^* = \omega\sqrt{\rho_i/M_i}$ the complex wave number in free stratified edge Ω_s (rectangular voids). It follows that the homogenized problems reads

$$
\begin{cases}
\dfrac{\partial^2 U^h}{\partial X_1^2} + K_i^{*2} U^h = 0 & \text{for } 0 < X_1 < e,\\
\Delta U^h + {K_R}^2 U^h = 0 & \text{for } X_1 > e,\\
\dfrac{\partial U^h}{\partial X_1}(0, X_2) = 0, & \\
\text{jump conditions(10)} & \text{at } X_1 = e,\\
\lim\limits_{X_1 \to +\infty} \left[\dfrac{\partial}{\partial X_1}\big(U^h - U^{\mathrm{inc}}\big) \mp \mathrm{i} K_R \cos\theta \big(U^h - U^{\mathrm{inc}}\big) \right] = 0, & \\
U^h \left(X_1, \dfrac{H}{2} \right) = e^{\mathrm{i} K_R \sin\theta} U^h \left(X_1, -\dfrac{H}{2} \right), & X_1 \in \mathbb{R}^+,\\
\dfrac{\partial U^h}{\partial X_2} \left(X_1, \dfrac{H}{2} \right) = e^{\mathrm{i} K_R \sin\theta} \dfrac{\partial U^h}{\partial X_2} \left(X_1, -\dfrac{H}{2} \right), & X_1 \in \mathbb{R}^+
\end{cases}
\tag{13}
$$

To obtain the effective parameters $(\mathcal{B}, \mathcal{C})$ entering in the jump conditions (10), we use the same method based on the modal methods (see S1 in [10]) for solving numerically the elementary problems (36) and (37) in the case of an array of rectangular voids. The solution of (13) with (11) is of the form

$$
\begin{cases}
U(\mathbf{X}) = \left[a\, \mathrm{e}^{\mathrm{i} K_i^* (X_1 - e)} + b\, \mathrm{e}^{-\mathrm{i} K_i^* (X_1 - e)} \right] \mathrm{e}^{\mathrm{i} K_R \sin\theta X_2}, & 0 < X_1 < e,\\
U(\mathbf{X}) = \left[\mathrm{e}^{-\mathrm{i} K_R \cos\theta (X_1 - e)} + R\, \mathrm{e}^{\mathrm{i} K_R \cos\theta (X_1 - e)} \right] \mathrm{e}^{\mathrm{i} K_R \sin\theta X_2}, & X_1 > e
\end{cases}
\tag{14}
$$

with (R, a, b) are given by using jump conditions (10) with (14). In particular, the reflection coefficient R reads

$$
R = \frac{z_1 \mathrm{e}^{-\mathrm{i} K_i^* e} - z_2^* \mathrm{e}^{\mathrm{i} K_i^* e}}{z_2 \mathrm{e}^{-\mathrm{i} K_i^* e} - z_1^* \mathrm{e}^{\mathrm{i} K_i^* e}},
\tag{15}
$$

with

$$
\begin{cases}
z_1 \equiv h K_R^2 \left(\mathcal{B} \cos\theta \sin\theta \phi\xi + \mathcal{C} \sin\theta^2 \right) + \mathrm{i} K_R \left(\cos\theta - \sin\theta \phi\xi \right) \left(\frac{1}{4} h^2 \mathcal{B}\mathcal{C} K_R^2 \sin\theta^2 + 1 \right),\\
z_2 \equiv h K_R^2 \left(\mathcal{B} \cos\theta \sin\theta \phi\xi - \mathcal{C} \sin\theta^2 \right) + \mathrm{i} K_R \left(\cos\theta + \sin\theta \phi\xi \right) \left(\frac{1}{4} h^2 \mathcal{B}\mathcal{C} K_R^2 \sin\theta^2 + 1 \right).
\end{cases}
$$

3.2.2. The case of stratified edge and substrate are the same viscoelastic media

In this second case, we consider $a^* = 1$, $b^* = (K^*/K_R)^2$ in the substrate, and φ the filling fraction of the substrate in the layers, the bulk parameters in the equivalent medium become $\langle a^* \rangle = \varphi$; $\langle b^* \rangle = (\frac{K^*}{K_R})^2 \varphi$ and $\langle 1/a^* \rangle^{-1} = 0$, whence the homogenized wave equation (30) reads

$$
\operatorname{div} \mathbf{\Sigma}^h + \varphi K^{*2} U^h = 0, \quad \mathbf{\Sigma}^h = \begin{pmatrix} \varphi & 0 \\ 0 & 0 \end{pmatrix} \boldsymbol{\nabla} U^h.
$$

It follows that the homogenized problems reads

$$
\begin{cases}
\dfrac{\partial^2 U^h}{\partial X_1^2} + K^{*2} U^h = 0, & \text{for } 0 < X_1 < e,\\
\Delta U^h + K^{*2} U^h = 0, & \text{for } X_1 > e,\\
\dfrac{\partial U^h}{\partial X_1}(0, X_2) = 0, & \\
\text{jump conditions (10)} & \text{at } X_1 = e,\\
\lim\limits_{X_1 \to +\infty} \left[\dfrac{\partial}{\partial X_1}\big(U^h - U^{\mathrm{inc}}\big) - \mathrm{i} K_S \big(U^h - U^{\mathrm{inc}}\big) \right] = 0, & \\
U^h \left(X_1, \dfrac{H}{2} \right) = \mathrm{e}^{\mathrm{i} K_{\mathrm{inc}}} U^h \left(X_1, -\dfrac{H}{2} \right), & X_1 \in \mathbb{R}^+,\\
\dfrac{\partial U^h}{\partial X_2} \left(X_1, \dfrac{H}{2} \right) = \mathrm{e}^{\mathrm{i} K_{\mathrm{inc}}} \dfrac{\partial U^h}{\partial X_2} \left(X_1, -\dfrac{H}{2} \right), & X_1 \in \mathbb{R}^+.
\end{cases}
\tag{16}
$$

The solution of (16) with (11) is of the form

$$\begin{cases} U(\mathbf{X}) = \left[a\mathrm{e}^{\mathrm{i}K^*(X_1-e)} + b\mathrm{e}^{-\mathrm{i}K^*(X_1-e)}\right]\mathrm{e}^{\mathrm{i}K_{\mathrm{inc}}X_2}, & 0 < X_1 < e \\ U(\mathbf{X}) = \left[\mathrm{e}^{-\mathrm{i}K_S(X_1-e)} + R\mathrm{e}^{\mathrm{i}K_S(X_1-e)}\right]\mathrm{e}^{\mathrm{i}K_{\mathrm{inc}}X_2}, & X_1 > e \end{cases} \tag{17}$$

with (R, a, b) are given by using jump conditions (10) with (17). In particular, the reflection coefficient R reads

$$R = \frac{z_1\mathrm{e}^{-\mathrm{i}K^*e} - z_2^*\mathrm{e}^{\mathrm{i}K^*e}}{z_2\mathrm{e}^{-\mathrm{i}K^*e} - z_1^*\mathrm{e}^{\mathrm{i}K^*e}}, \tag{18}$$

with

$$\begin{cases} z_1 \equiv h\left(\mathcal{B}K_SK_{\mathrm{inc}}\phi\xi + \mathcal{C}{K_{\mathrm{inc}}}^2\right) + \mathrm{i}\left(K_S - K_{\mathrm{inc}}\phi\xi\right)\left(\frac{1}{4}h^2\mathcal{B}\mathcal{C}{K_{\mathrm{inc}}}^2 + 1\right), \\ z_2 \equiv h\left(\mathcal{B}K_SK_{\mathrm{inc}}\phi\xi - \mathcal{C}{K_{\mathrm{inc}}}^2\right) + \mathrm{i}\left(K_S + K_{\mathrm{inc}}\phi\xi\right)\left(\frac{1}{4}h^2\mathcal{B}\mathcal{C}{K_{\mathrm{inc}}}^2 + 1\right). \end{cases}$$

3.3. Accuracy of the homogenized solution with respect to the actual solution

To validate the homogenized problem, we report the fields U^{num} calculated numerically and the fields U of the homogenized solutions in the case of welded viscoelastic stratified edge with elastic substrate (14)–(15), for $\varphi = 0.5$ and $\varphi = 0.9$ (Figure 5); in both cases, the reciprocal quality factor $Q_m^{-1} = 0$ for elastic substrate and $Q_{in}^{-1} = 0.1$ for viscoelastic free stratified edge Ω_s, with $K_Rh = 1$, $e/h = 10$ and $\theta = \pi/3$. For the problem of stratified edge and substrate are considered the same viscoelastic media (14)–(15), we reported the fields U^{num} and U for reciprocal quality factors $Q^{-1} = 0.05$ in the Low-Loss viscoelastic media ($Q^{-1} \ll 1$), and for no Low-Loss media $Q^{-1} = 0.2$; in both cases, $K_Rh = 1$, $e/h = 10$, $\varphi = 0.5$, $\theta = \pi/3$, and $\gamma = \pi/6$. Defining $\Delta U \equiv \|U - U^{\mathrm{num}}\| / \|U^{\mathrm{num}}\|$ (for $|X_1| > e/2$ and with $\|\cdot\|$ the L^2 norm), we get a discrepancy of 0.5% ($\varphi = 0.5$) and 0.8% ($\varphi = 0.9$) for the first case, and almost the same discrepancy 0.5% ($Q^{-1} = 0.05$) and 0.7% ($Q^{-1} = 0.2$) for the second case, where the substrate and stratified edge are the same viscoelastic media. It is interesting to note that a very small error is found even if the value $kh = 1$ is relatively large.

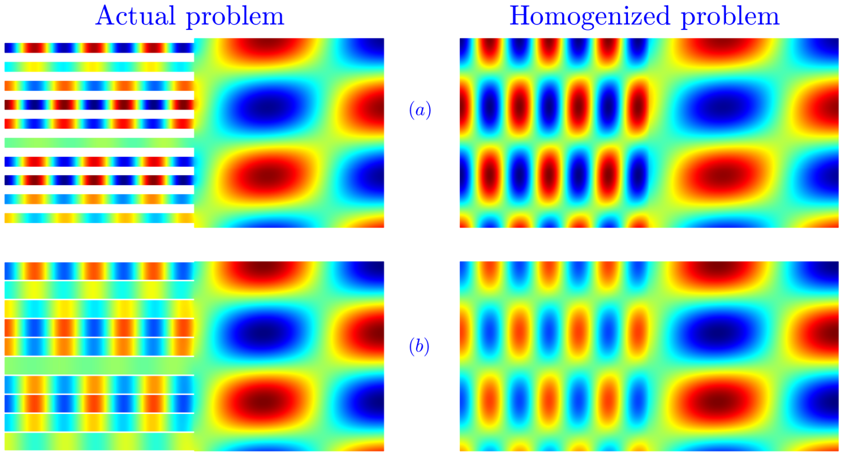

Fig. 5. (a) The numerical solution U^{num} in the actual problem for an oblique incident plane wave $\theta = \pi/3$ with degree of inhomogeneity $\gamma = \pi/6$ and $K_Rh = 1$, on a welded elastic substrate $Q_m^{-1} = 0$ with viscoelastic stratified edge $Q_{\mathrm{in}}^{-1} = 0.1$ made of rectangular voids ($e/h = 10$ and $\varphi = 0.5$); the right shows the homogenized fields U. (b) Same representation as (a) with $\varphi = 0.9$.

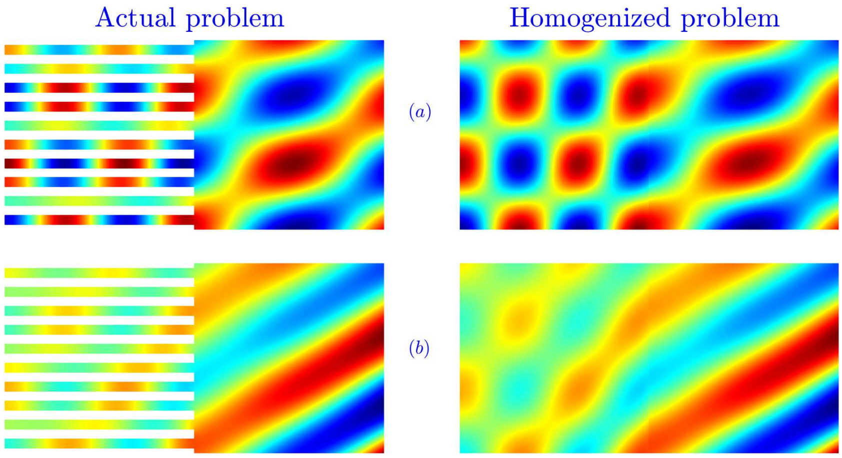

Fig. 6. (a) Same representation as in Figure 5 for a case of the stratified edge and substrate are the same viscoelastic media ($Q^{-1} = 0.05$ with $\varphi = 0.5$). (b) Same representation as (a) with $Q^{-1} = 0.2$ in the case of no Low-Loss viscoelastic media.

3.3.1. The error of the reflection as a function of frequencies

In the first time, we shall inspect for $Q_m^{-1} = 0$ and $Q_{in}^{-1} = 0.1$ in the case of welded viscoelastic stratified edge with elastic substrate, for which we report reflection coefficients R^{num} and R as a function of kh and e/h (with $\varphi = 0.1$, $\theta = \pi/3$ and $\gamma = \pi/6$), and the corresponding errors $\Delta R = |R^{\mathrm{num}} - R| \,/\, |R^{\mathrm{num}}|$. We considered $K_R h \in [0, 2\pi]$, where the frequency range includes $K_R h > 2\pi/(1+\sin\theta) \simeq 1.07\pi$, corresponding to the Wood anomaly (cut-off frequency) [16]. This interval is outside the range of validity of any homogenization approach, whereas mode coupling is not possible at an equivalent flat boundary.

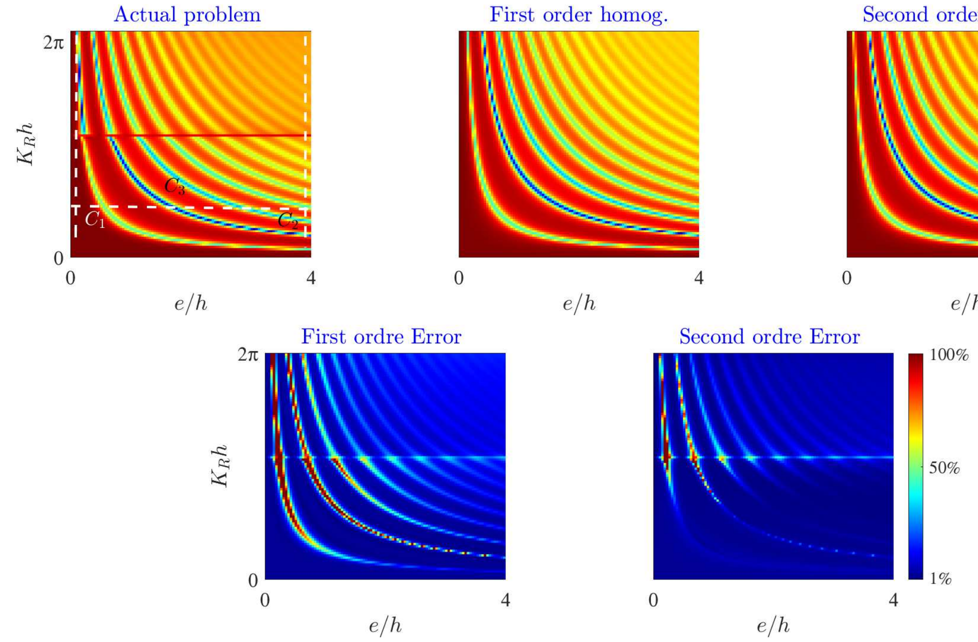

Fig. 7. Up: Reflection coefficients in actual problem $|R^{\mathrm{num}}|$ and homogenized $|R|$ at the first order ($\mathcal{B} = \mathcal{C} = 0$), and at the second order as a function of e/h and of the frequency $K_R h$; ($Q_m^{-1} = 0$, $Q_{in}^{-1} = 0.1$, $\varphi = 0.1$, $\theta = \pi/3$ and $\gamma = \pi/6$) have been considered. Down: Errors ΔR on the reflection coefficient, which are calculated numerically. Errors smaller than 1% appear in dark blue, and errors greater than 100% appear in dark red.

In Figure 7, errors smaller than 1% appear in dark blue, and errors greater than 100% appear in dark red. On average, at the intermediate frequencies for $K_R h < \pi/2$ (C_3 profile), the error in the reflection coefficient for $Q^{-1} = 0.1$, is smaller than 1% in the whole range of e/h at the second order, and it is of 50% on average at the first order ($\mathcal{B} = \mathcal{C} = 0$); on the other hand, the first order homogenization wrongly predicts perfect reflections for e/h for vanishing thicknesses e/h, while including the jump conditions (10) at the second order restores the real scattering properties of an array of flat voids. This is corresponding to the result of [17], in which the effective permittivity of electromagnetic waves must depend on the thickness (the effective bulk parameter a in our case).

More precisely, we inspect (i) for a small thickness (C_1 profile from Figure 7) the profiles of $|R^{\mathrm{num}}|$ (blue symbols) and its homogenized reflection coefficient $|R|$ (grey lines at the first order and black lines at the second order), with the corresponding errors ΔR (grey lines at the first order and black liens at the second) as a function of kh for $e/h = 0.05$ and $e/h = 4$ (Figure 8). We notice that the homogenization at the first order largely overestimates the reflection, while the homogenization at the second order recovers the actual reflection of the stratified edge; for a larger free stratified edge (C_2 profile) the first order homogenization is valid for small $K_R h$; and going up to the second order allows us to enlarge the interval of validity of the homogenized solution. (ii) The variations of $|R^{\mathrm{num}}|$ and $|R|$ (and the corresponding errors ΔR) as a function of e/h for $K_R h = 0.6\pi$ are reported in Figure 9 (C_3 profile from Figure 7). We note that the homogenized solution at the second order is even more significant than that at the first order.

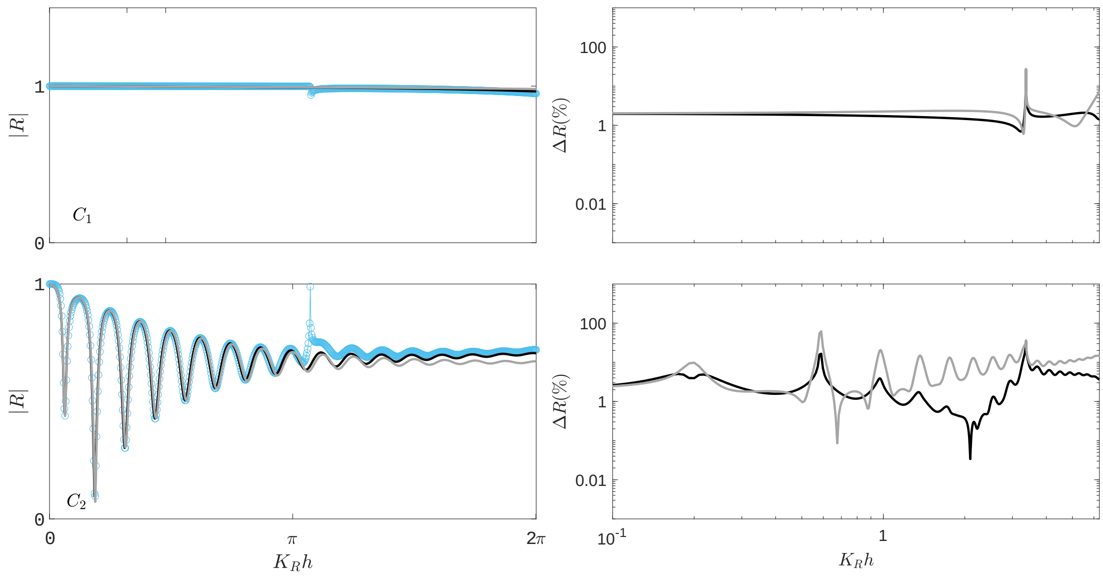

Fig. 8. Left: Reflection coefficients $|R^{\text{num}}|$ and $|R|$ as a function of $K_R h$. C_1 profile for $e/h = 0.05$ and C_2 for $e/h = 4$ ($|R^{\text{num}}|$: blue symbols and $|R|$: grey lines at the first order and black lines at the second order). Right: The corresponding error ΔR of the homogenized predictions, which are shown in percent (grey lines at the first order and black liens at the second).

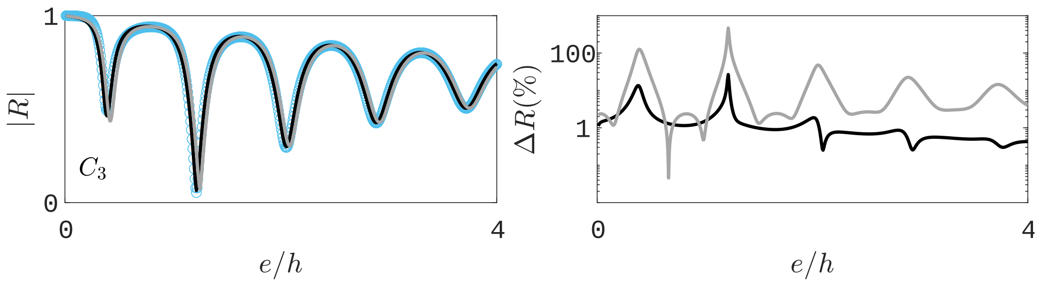

Fig. 9. Reflection coefficients $|R^{\text{num}}|$ and $|R|$ and errors ΔR as a function of e/h for $K_R h = 0.6\pi$ (C_3 profile from Figure 7). Same representation as in Figure 8.

3.3.2. The error of the reflection as a function of reciprocal quality factor

Finally, we report the reflection coefficients R^{num} and R as a function of $K_R h$ and the reciprocal quality factor Q^{-1} (with $e/h = 4$, $\varphi = 0.1$, $\theta = \pi/3$ and $\gamma = \pi/6$), and the corresponding errors ΔR Figure 10. We considered $K_R h \in [0, 2\pi]$, $K_R h \simeq 1.07\pi$ corresponding to the cut-off frequency exists in the actual problem.

In Figure 10, errors smaller than 1% appear in dark blue, and errors greater than 100% appear in dark red. On average, at the intermediate frequencies for $K_R h < \pi/2$ (C_0 profile), the error in the reflection coefficient is smaller than 1% in the whole range of Q^{-1}; it is of 25% on average at the first order. More specifically, we inspect the variations of $|R^{\text{num}}|$ (blue symbols) and its homogenized reflection coefficient $|R|$ (grey lines at the first order and black lines at the second order), with the corresponding error ΔR (grey lines at the first order and black liens at the second) as a function of the reciprocal quality factor Q_{in}^{-1} of a stratified edge (Figure 11). For the case of the welded elastic substrate with a viscoelastic stratified edge with ($Q_m^{-1} = 0$, $K_R h = 0.6\pi$) and ($e/h = 4$, $\varphi = 0.1$, $\theta = \pi/3$). Also, the first order homogenization underestimates the scattering properties of the structure, the homogenized solution at the second order is valid for $K_R h = 0.6\pi$ by noting that the ΔR error is less than 1% in the whole range of Q^{-1}.

Finally, we inspected the variations of $|R^{\text{num}}|$ as a function of the reciprocal quality factor Q_m^{-1} of a substrate (Figure 11), in the event that free stratified edge and a substrate are two different viscoelastic media, with $Q_{in}^{-1} = 0.2$ and ($K_R h = 0.6\pi$, $e/h = 4$, $\varphi = 0.1$, $\theta = \pi/3$, $\gamma = \pi/6$). The homogenized solution is also valid by noting that the ΔR error is less than 1% in the whole range of Q_m^{-1}. We obtain almost the same results as those observed in the other cases, and in general the homogenized solution at the second order is even more significant than that at the first order.

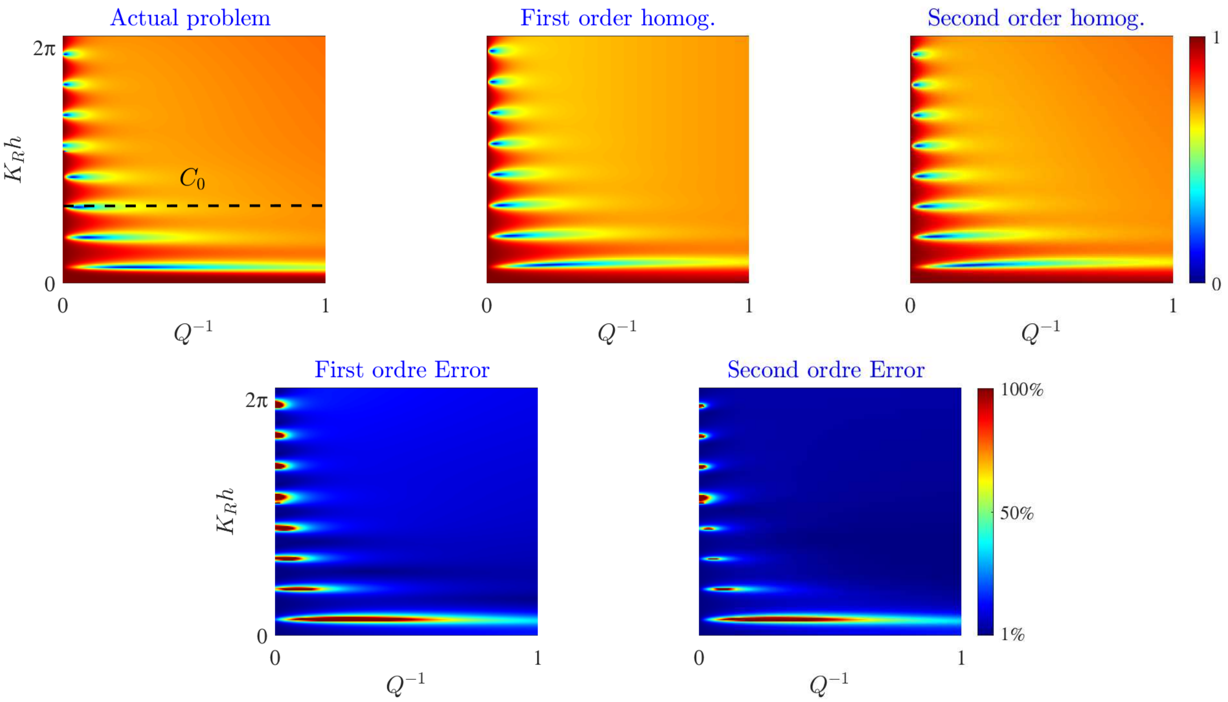

Fig. 10. Up: Reflection coefficients in actual problem $|R^{\text{num}}|$ and homogenized $|R|$ at the first order ($\mathcal{B} = \mathcal{C} = 0$), and at the second order as a function of Q^{-1} and of the frequency $K_R h$; with ($e/h = 4$, $\varphi = 0.1$, $\theta = \pi/3$ and $\gamma = \pi/6$). Down: Errors ΔR on the transmission coefficient, which are calculated numerically. Errors smaller than 1% appear in dark blue, and errors greater than 100% appear in dark red.

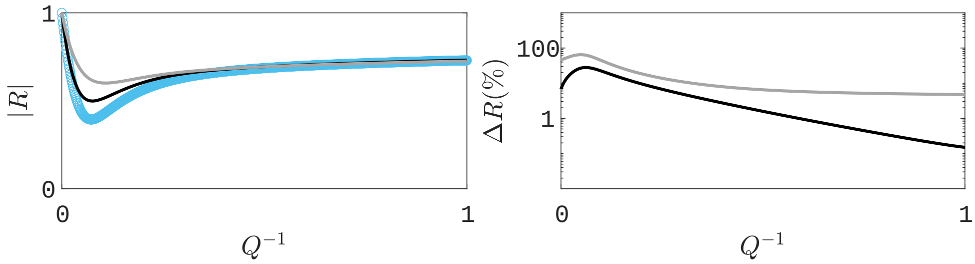

Fig. 11. Up: Reflection coefficients $|R^{\text{num}}|$ (blue symbol), $|R|$ (grey lines at the first order and black lines at the second order) and errors ΔR (grey lines at the first order and black liens at the second) as a function of Q_{in}^{-1} for elastic substrate ($Q_m^{-1} = 0$, $K_R h = 0.6\pi$), with ($e/h = 4$, $\varphi = 0.1$, $\theta = \pi/3$). Down: Same representation as a function of Q_m^{-1} for viscoelastic substrate ($Q_{in}^{-1} = 0.1$, $K_R h = 0.6\pi$), with ($e/h = 4$, $\varphi = 0.1$, $\theta = \pi/3$ and $\gamma = \pi/6$).

4. Concluding remarks

In this work, we have presented a homogenization model able to replace the physical problem of the scattering of shear waves at a welded viscoelastic substrate with a free viscoelastic stratified edge. The problem ends with effective parameters characteristic of an equivalent anisotropic free slab and which enter in jump conditions for the displacement and the normal stress at the welded boundaries between a substrate and stratified edge. As in classical homogenization, these effective parameters are obtained by the solutions of elementary problems. The most significant simplicity in the presented approach is the derivation of effective bulk parameters which are simply averages of the bulk parameters in each layer, and these effective bulk parameters enter in the homogenized wave equation. The method has been presented in the case of rectangular voids spaced periodically on the surface of a viscoelastic substrate and associated with Neumann boundary conditions. In acoustics, this corresponds to an array of sound hard material in a fluid, in electromagnetism to a (perfect conducting) metallic array in a dielectric or in the air. The model accurately describes the spectra of reflection thanks to an explicit expression of the reflection coefficients deduced from the effective interface parameters, this accuracy has specifically been shown for the Low-Loss viscoelastic media and no Low-Loss media, with a range of validity being $K_R h < \pi/2$. While the frequency range includes $K_R h \simeq 1.07\pi$, corresponding to the Wood anomaly. This range is outside the range of validity of any homogenization approach, since mode coupling is not possible at an equivalent flat boundary.

Acknowledgments

The authors thank the anonymous reviewers for their insightful comments and suggestions.

Appendix A. Effective problem in the region of the welded boundary

Fig. 12. Left: configuration in the x coordinate; the periodicity along x_2 is $\varepsilon \equiv K_R h$; the inner region corresponds to the neighborhood of the boundary between the stratified medium ($x_1 < 0$) and the substrate being a homogeneous medium ($x_1 > 0$). Right: the unit cell (inner region) in the y coordinate, with $\mathbf{y} = \mathbf{x}/\varepsilon$, and $\mathbf{y} \in \mathbb{R} \times Y$, with $Y = (-1/2, 1/2)$.

Let us derive the effective model for two viscoelastic media of a free stratified edge and an infinite substrate with a common interface boundary in welded contact. From the position of physical problems (7)–(8), we noticed that the wave equation is identical to the one homogenized in [9, 10], except that in our case, the coefficients of physical parameters entering the equation wave are complex. Therefore, we obtained by analogy the same form of the homogenized wave equations at different orders; for this reason, we will quote in this work, only the main steps of this derivation.

A.1. The matched asymptotic expansion

As previously said, we shall apply the same asymptotic expansions technique as in [9] by spearing the space into three regions.

A.1.1. Inner and outer expansions

The inner region contains the boundary between the stratified medium and the substrate (Figure 12). Two outer regions for $x_1 > 0$ and $x_1 < 0$ are the regions far enough from the interface, where the evanescent field can be neglected. Next, the inner region and the outer regions are connected using so-called matching conditions, which will constitute the boundary conditions for the outer solutions. Owing to this approach, the expansions reads

$$\begin{cases} \text{outer region } x_1 > 0, & u^\varepsilon = u^0(\mathbf{x}) + \varepsilon u^1(\mathbf{x}) + \cdots \\ & \sigma^\varepsilon = \sigma^0(\mathbf{x}) + \varepsilon \sigma^1(\mathbf{x}) + \ldots, \\ \text{outer region } x_1 < 0, & u^\varepsilon = u^0(\mathbf{x}, y_2) + \varepsilon u^1(\mathbf{x}, y_2) + \ldots, \\ & \sigma^\varepsilon = \sigma^0(\mathbf{x}, y_2) + \varepsilon \sigma^1(\mathbf{x}, y_2) + \ldots, \\ \text{inner region,} & u^\varepsilon = v^0(x_2, \mathbf{y}) + \varepsilon v^1(x_2, \mathbf{y}) + \ldots, \\ & \sigma^\varepsilon = \tau^0(x_2, \mathbf{y}) + \varepsilon \tau^1(x_2, \mathbf{y}) + \ldots. \end{cases} \tag{19}$$

With the outer terms (u^n, σ^n) for $x_1 < 0$ and the inner terms (v^n, τ^n) being Y periodic with $Y = (-1/2, 1/2)$; and now, the second actual problem (5) can be written in the inner and in the outer regions, owing to the expressions of the differential operator

$$\begin{cases} \text{in the outer region,} & \nabla \to \nabla_{\mathbf{x}}, & x_1 > 0, \\ & \nabla \to \nabla_{\mathbf{x}} + \dfrac{1}{\varepsilon}\dfrac{\partial}{\partial y_2}\mathbf{e}_2, & x_1 < 0, \\ \text{in the inner region,} & \nabla \to \dfrac{\partial}{\partial x_2}\mathrm{e}_2 + \dfrac{1}{\varepsilon}\nabla_{\mathbf{y}}, & \end{cases} \tag{20}$$

where $\nabla_{\mathbf{x}}$ and $\nabla_{\mathbf{y}}$ means gradient with respect to $\mathbf{x}$ and $\mathbf{y}$ respectively, such as a macroscopic coordinate $\mathbf{x}$ associated with slow variations of the fields (with the typical scale $1/K_R$ of the wave) and a microscopic coordinate $\mathbf{y} \equiv \mathbf{x}/\varepsilon$, associated with rapid variations (the typical scale h of the layers), and in each region, we keep the coordinates that are relevant to describe the variations of the field.

Finally, from (6), $(a^{*\varepsilon}, b^{*\varepsilon})$ can be specified in the outer regions as

$$\begin{cases} \text{outer region } x_1 > 0, & a^{*\varepsilon}(\mathbf{x}) = 1, & b^{*\varepsilon}(\mathbf{x}) = \left(K^*/K_R\right)^2, \\ \text{outer region } x_1 < 0, & a^{*\varepsilon}(\mathbf{x}) = a^*\left(x_2/\varepsilon\right), & b^{*\varepsilon}(\mathbf{x}) = b^*\left(x_2/\varepsilon\right), \end{cases} \tag{21}$$

and in the inner region as $a^{*\varepsilon}(\mathbf{x}) = \tilde{a^*}(\mathbf{x}/\varepsilon)$ and $b^{*\varepsilon}(\mathbf{x}) = \tilde{b^*}(\mathbf{x}/\varepsilon)$ with

$$\tilde{a^*}(\mathbf{y}) = \begin{cases} a^*\left(y_2\right), & y_1 < 0, \\ 1, & y_1 > 0, \end{cases} \quad \tilde{b^*}(\mathbf{y}) = \begin{cases} b^*\left(y_2\right), & y_1 < 0, \\ \left(K^*/K_R\right)^2, & y_1 > 0, \end{cases} \tag{22}$$

with $a^*(y_2)$, $b^*(y_2)$ 1-periodic and piecewise complex constant.

A.1.2. Matching conditions

Because of the separation of the space into two regions, something has to be said on the boundary conditions at $|y_1| \to +\infty$ and for $x_1 \to 0^{\pm}$, which are unknown a priori. It is in fact these boundary conditions that will provide the jump conditions. The missing conditions for the inner and outer terms are given simultaneously by so-called matching conditions, which tell us that two solutions have to match in some intermediate region. Following [18] the matching is written for $x_1 \to 0^{\pm}$ corresponding to $y_1 \to \pm\infty$ (and we denote $f\left(0^{\pm}\right)$ the limit values of f for $x_1 \to 0^{\pm}$). To do so, we use the Taylor expansions of $u^0\left(x_1, x_2\right) = u^0\left(0^{\pm}, x_2\right) + x_1 \partial_{x_1} u^0\left(0^{\pm}, x_2\right) + \ldots = u^0\left(0^{\pm}, x_2\right) + \varepsilon y_1 \partial_{x_1} u^0\left(0^{\pm}, x_2\right) + \ldots$, same for σ^0. Identifying the terms in ε^n, $n = 0, 1$ in the inner and outer expansions (19), we get, for $n = 0$

$$\begin{cases} u^0(0^-, x_2, y_2) = \lim\limits_{y_1 \to -\infty} v^0(x_2, y), & \text{(23a)} \\ u^0(0^+, x_2) = \lim\limits_{y_1 \to +\infty} v^0(x_2, y), & \text{(23b)} \\ \sigma^0(0^-, x_2, y_2) = \lim\limits_{y_1 \to -\infty} \tau^0(x_2, y), & \text{(23c)} \\ \sigma^0(0^+, x_2) = \lim\limits_{y_1 \to +\infty} \tau^0(x_2, y), & \text{(23d)} \end{cases}$$

and for $n = 1$

$$\begin{cases} u^1(0^-, x_2, y_2) = \lim\limits_{y_1 \to -\infty} \left[y^1(x_2, \mathbf{y}) - y_1 \dfrac{\partial u^0}{\partial x_1}(0^-, x_2, y_2)\right], & \text{(24a)} \\ u^1(0^+, x_2) = \lim\limits_{y_1 \to +\infty} \left[y^1(x_2, \mathbf{y}) - y_1 \dfrac{\partial u^0}{\partial x_1}(0^+, x_2)\right], & \text{(24b)} \\ \sigma^1(0^-, x_2, y_2) = \lim\limits_{y_1 \to -\infty} \left[\tau^1(x_2, \mathbf{y}) - y_1 \dfrac{\partial \sigma^0}{\partial x_1}(0^-, x_2, y_2)\right], & \text{(24c)} \\ \sigma^1(0^+, x_2) = \lim\limits_{y_1 \to +\infty} \left[\tau^1(x_2, \mathbf{y}) - y_1 \dfrac{\partial \sigma^0}{\partial x_1}(0^+, x_2)\right]. & \text{(24d)} \end{cases}$$

A.2. The homogenized wave equations

We shall start by reporting directly, the outer and inner solution at the first and the second orders, that will be needed to generate the wave equation, up to the second order, satisfied by the mean fields $(\bar{u}(\mathbf{x}), \bar{\sigma}(\mathbf{x}))$ with

$$\bar{u} \equiv \left\langle u^0 \right\rangle + \varepsilon \left\langle u^1 \right\rangle, \quad \bar{\sigma} \equiv \left\langle \sigma^0 \right\rangle + \varepsilon \left\langle \sigma^1 \right\rangle. \tag{25}$$

We note that if f does not depend on $y_2, \langle f \rangle = f$, and using (19) to (22) in actual wave equations (5). We obtain the homogenized wave equations at the first and the second orders, in the following forms.

A.2.1. Outer solutions

For $x_1 > 0$, at the first and the second order $(n = 0, 1)$

$$\begin{cases} \operatorname{div}_{\mathbf{x}} \boldsymbol{\sigma}^n + \left(\dfrac{K^*}{K_R} \right)^2 u^n = 0, \\ \boldsymbol{\sigma}^n = \boldsymbol{\nabla}_{\mathbf{x}} u^n. \end{cases} \tag{26}$$

A.2.2. Inner solutions

For $x_1 < 0$, reads

$$\text{at order } \varepsilon^{-1}\colon \begin{cases} u^0(\mathbf{x}, y_2) = u^0(\mathbf{x}), \\ \sigma_2^0(\mathbf{x}, y_2) = \sigma_2^0(\mathbf{x}); \end{cases} \tag{27}$$

$$\text{at order } \varepsilon^{0}\colon \begin{cases} \operatorname{div}_{\mathbf{x}} \left\langle \sigma^0 \right\rangle + \langle b^* \rangle u^0 = 0, \\ \left\langle \sigma^0 \right\rangle (\mathbf{x}) = \langle a^* \rangle \dfrac{\partial u^0}{\partial x_1}(\mathbf{x}) \mathbf{e}_1 + \langle 1/a^* \rangle^{-1} \dfrac{\partial u^0}{\partial x_2}(\mathbf{x}) \mathbf{e}_2; \end{cases} \tag{28}$$

$$\text{at order } \varepsilon^{1}\colon \begin{cases} \operatorname{div}_{\mathbf{x}} \left\langle \boldsymbol{\sigma}^1 \right\rangle (\mathbf{x}) + \langle b^* \rangle \left\langle u^1 \right\rangle (\mathbf{x}) = 0, \\ \left\langle \sigma_1^1 \right\rangle (\mathbf{x}) = \langle a^* \rangle \dfrac{\partial \left\langle u^1 \right\rangle}{\partial x_1}(\mathbf{x}), \quad \left\langle \sigma_2^1 \right\rangle (\mathbf{x}) = \langle 1/a^* \rangle^{-1} \dfrac{\partial \left\langle u^1 \right\rangle}{\partial x_2}(\mathbf{x}). \end{cases} \tag{29}$$

We got (29) at order ε^1 thanks to two following relations demonstrated in [9] (see subsection 2.2.2)

$$\left\langle f(\cdot) u^1(\mathbf{x}, \cdot) \right\rangle = \langle f \rangle \left\langle u^1 \right\rangle (\mathbf{x}) \text{ and } \left\langle f(\cdot) \sigma_2^1(\mathbf{x}, \cdot) \right\rangle = \langle f \rangle \left\langle \sigma_2^1 \right\rangle (\mathbf{x}) \quad \text{for any even } f.$$

Both relations use the same property: consider a piecewise differentiable function $g(y)$, with $g'(y)$ even; then $(g - \langle g \rangle)$ is odd, and for any function $f(y)$ being even, $f(g - \langle g \rangle)$ is odd. Finally, to determine the homogenized wave equation up to the second order for $(\bar{u}(\mathbf{x}), \bar{\sigma}(\mathbf{x}))$, it is enough to apply (26), (28) and (29) in (25)

$$\operatorname{div} \bar{\sigma} + \langle b^* \rangle \bar{u} = 0, \quad \bar{\sigma} = \begin{pmatrix} \langle a^* \rangle & 0 \\ 0 & \langle 1/a^* \rangle^{-1} \end{pmatrix} \nabla \bar{u} \quad \text{for} \quad x_1 < 0. \tag{30}$$

Next, (26) to (29) with the boundary conditions and the matching conditions will be used to find the conditions to be applied on an equivalent interface at $x_1 = 0$, so-called jump condition.

A.3. The jump conditions and interface parameters

We start with the jump conditions at the first order $[\![v^0]\!]$ and $[\![\sigma_1^0]\!]$.

A.3.1. Jump conditions at the first order

The actual wave equations (5) for the inner problem at the leading order in ε^{-1} give

$$\nabla_{\mathbf{y}} v^0 = 0, \quad \operatorname{div}_y \tau^0 = 0,$$

from which we deduce that v^0 does not depend on $\mathbf{y}$. With (27), $u^0(\mathbf{x})$ does not depend too on y_2, thus

$$u^0(0^-, x_2) = u^0(0^+, x_2) = v^0(x_2). \tag{31}$$

Next, integrating $\mathrm{div}_y\, \tau^0 = 0$ over $\mathbb{R} \times Y$ (Figure 13), and using (i) the continuity of $\tau^0 \cdot \mathbf{n}$ between the layers along y_2, and (ii) the periodicity of τ^0 with respect to y_2, we get

$$\int_Y \mathrm{d}y_2 \left[\tau_1^0(x_2, +\infty, y_2) - \tau_1^0(x_2, -\infty, y_2)\right] = 0.$$

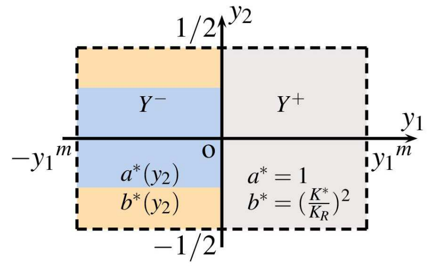

Fig. 13. The domain $\mathbf{Y} = Y^- \cup Y^+$, with $Y^- = (-y_1^m, 0) \times Y$, $Y^+ = (0, +y_1^m) \times Y$. $\tilde{a}^*(\mathbf{y}) = a^*(y_2)$ and $\tilde{b^*}(\mathbf{y}) = b^*(y_2)$ in Y^-, and $a = 1$, $b = \left(K^*/K_R\right)^2$ in Y^+.

Finally, integrating the matching condition (23c) and (23d) over Y, we get

$$\left\langle \sigma_1^0 \right\rangle (0^-, x_2) = \sigma_1^0(0^+, x_2). \tag{32}$$

By using (9), we deduce from (31)–(32) the jump conditions at the first order

$$[\![u^0]\!] = [\![\langle \sigma_1^0 \rangle]\!] = 0. \tag{33}$$

From(33), we note that the normal displacement and stress are continued, which requires us to go up to the second order to capture the effect of boundary layers at $x_1 = 0$.

In order to obtain the jump conditions at the second order, we need to find the solutions of the elementary problems.

A.3.2. The elementary problems

From the first equation in (5) at order ε^{-1} and the second equation in (5) at order ε^0, the matching conditions (23c)–(23d), it follows that the system satisfied by $v^1(x_2, \mathbf{y})$ can be written

$$\begin{cases} \mathrm{div}_{\mathbf{y}}\, \tau^0 = 0 \quad \text{with} \quad \tau^0 = \tilde{a^*}(\mathbf{y}) \left[\dfrac{\partial u^0}{\partial x_2}(0, x_2)\mathbf{e}_2 + \nabla_{\mathbf{y}} v^1(x_2, \mathbf{y})\right], \\ v^1 \text{ and } \tau^0 \cdot \mathbf{n} \text{ continuous}, \\ \displaystyle\lim_{y_1 \to -\infty} \nabla_{\mathbf{y}} v^1(x_2, \mathbf{y}) = \langle a^* \rangle^{-1} \left\langle \sigma_1^0 \right\rangle (0, x_2)\mathbf{e}_1 + \frac{1/a^*(y_2) - \langle 1/a^* \rangle}{\langle 1/a^* \rangle} \frac{\partial u^0}{\partial x_2}(0, x_2)\mathbf{e}_2, \\ \displaystyle\lim_{y_1 \to +\infty} \nabla_{\mathbf{y}} v^1(x_2, \mathbf{y}) = \left\langle \sigma_1^0 \right\rangle (0, x_2)\mathbf{e}_1, \end{cases} \tag{34}$$

with v^1 and τ^0 periodic with respect to y_2. The system (34) is linear with respect to $\left\langle \sigma_1^0 \right\rangle (0, x_2)$ and $\partial_{x_2} u^0(0, x_2)$. Thus, we define $V^{(1)}(\mathbf{y})$ and $V^{(2)}(\mathbf{y})$ such that

$$\begin{cases} v^1(x_2, \mathbf{y}) = \left\langle \sigma_1^0 \right\rangle (0, x_2) V^{(1)}(\mathbf{y}) + \dfrac{\partial u^0}{\partial x_2}(0, x_2) \left[A^*(y_2) + V^{(2)}(\mathbf{y})\right] + \hat{v}(x_2), \\ \tau^0(x_2, \mathbf{y}) = \left\langle \sigma_1^0 \right\rangle (0, x_2)\mathbf{T}^{(1)}(\mathbf{y}) + \dfrac{\partial u^0}{\partial x_2}(0, x_2) \left[\dfrac{\tilde{a^*}(\mathbf{y})/a^*(y_2)}{\langle 1/a^* \rangle}\mathbf{e}_2 + \mathbf{T}^{(2)}(\mathbf{y})\right], \end{cases} \tag{35}$$

with

$$A^*(y_2) \equiv \int_{-1/2}^{y_2} \mathrm{d}y \frac{1/a^*(y) - \langle 1/a^* \rangle}{\langle 1/a^* \rangle}.$$

And

$$\mathbf{T}^{(1)}(\mathbf{y}) \equiv \tilde{a^*}(\mathbf{y}) \nabla V^{(1)}(\mathbf{y}), \quad \mathbf{T}^{(2)}(\mathbf{y}) \equiv \tilde{a^*}(\mathbf{y}) \nabla V^{(2)}(\mathbf{y}).$$

We notice that the field v^1 in (34) is defined up to a function of x_2, and it is denoted $\hat{v}(x_2)$ in (35); we shall see that the determination of $\hat{v}(x_2)$ is not needed. It is easy to see that if $\left(V^{(1)}, \mathbf{T}^{(1)}\right)$ satisfy the elementary problems,

$$
\begin{cases}
\operatorname{div} \mathbf{T}^{(1)} = 0 \quad \text{with} \quad \mathbf{T}^{(1)}(\mathbf{y}) = \tilde{a^*}(\mathbf{y}) \nabla V^{(1)}(\mathbf{y}), \\
V^{(1)} \quad \text{and} \quad \mathbf{T}^{(1)} \cdot \mathbf{n} \text{ continuous}, \\
V^{(1)}, \mathbf{T}^{(1)} \quad \text{periodic with respect to} \quad y_2, \\
\lim\limits_{y_1 \to -\infty} \nabla V^{(1)}(\mathbf{y}) = \dfrac{\mathbf{e}_1}{\langle a^* \rangle}, \quad \lim\limits_{y_1 \to +\infty} \nabla V^{(1)}(\mathbf{y}) = \mathbf{e}_1,
\end{cases}
\tag{36}
$$

and

$$
\begin{cases}
\operatorname{div} \left[\mathbf{T}^{(2)} + \dfrac{\tilde{a^*}(\mathbf{y})/a^*(y_2)}{\langle 1/a^* \rangle} \mathbf{e}_2 \right] = 0 \quad \text{with} \quad \mathbf{T}^{(2)}(\mathbf{y}) = \tilde{a^*}(\mathbf{y}) \nabla V^{(2)}(\mathbf{y}), \\
V^{(2)} \quad \text{and} \quad \left[\mathbf{T}^{(2)} + \dfrac{\tilde{a^*}(\mathbf{y})/a^*(y_2)}{\langle 1/a^* \rangle} \mathrm{e}_2 \right] \cdot \mathbf{n} \quad \text{continuous}, \\
V^{(2)}, \mathbf{T}^{(2)} \quad \text{periodic with respect to} \quad y_2, \\
\lim\limits_{y_1 \to -\infty} \nabla V^{(2)}(\mathbf{y}) = 0, \quad \lim\limits_{y_1 \to +\infty} \nabla V^{(2)}(\mathbf{y}) = -\dfrac{1/a^*(y_2) - \langle 1/a^* \rangle}{\langle 1/a^* \rangle} \mathrm{e}_2,
\end{cases}
\tag{37}
$$

then $v^1(x_2, \mathbf{y})$ satisfies (34). Next, by integrating the limits of $\nabla V^{(i)}$, $(i = 1, 2)$, with $V^{(i)}$ are defined up to a constants in (36) and (37), we can write

$$
\begin{cases}
\lim\limits_{y_1 \to -\infty} \left[V^{(1)} - \dfrac{y_1}{\langle a^* \rangle} \right] = -\mathcal{B}, \\
\lim\limits_{y_1 \to +\infty} \left[V^{(1)} - y_1 \right] = 0,
\end{cases}
\qquad
\begin{cases}
\lim\limits_{y_1 \to -\infty} V^{(2)} = -\mathcal{B}', \\
\lim\limits_{y_1 \to +\infty} V^{(2)} = -A^*(y_2).
\end{cases}
\tag{38}
$$

Such as, we denoted by $-\mathcal{B}$ (it is the first interface parameter) and $-\mathcal{B}'$ the constants at $y_1 \to -\infty$ for $V^{(1)}$ and $V^{(2)}$ respectively. Next, $V^{(2)}$ being odd with respect to y_2, we have $\mathcal{B}' = 0$. Finally, since the unknown constants being a priori different at $y_1 \to \pm\infty$, we can set these constants equal zero at $y_1 \to +\infty$ for $V^{(1)}$ and $V^{(2)}$.

A.3.3. Jump conditions at the second order

In order to find $\langle u^1 \rangle$ and $\langle \sigma_1^1 \rangle$, one can use the same steps followed in [9] (see subsection 2.3.3), which leads to obtain the following results

$$
[\![\langle u^1 \rangle]\!] = \mathcal{B} \left\langle \sigma_1^0 \right\rangle (0, x_2). \tag{39}
$$

And

$$
[\![\langle \sigma_1^1 \rangle]\!] = -\mathcal{C} \frac{\partial^2 u^0}{\partial x_2^2}(0, x_2). \tag{40}
$$

With $\mathcal{C} \equiv \int_Y \mathrm{d}\mathbf{y}\, T_2^{(2)}(\mathbf{y})$ is the second interface parameter.

A.3.4. Up to the second order jump conditions

Finally, we use (25) and (9) to obtain the final jumps on $\bar{u}$ and $\bar{\sigma}$, as follow

$$
[\![\bar{u}]\!] = [\![\langle u^0 \rangle]\!] + \varepsilon [\![\langle u^1 \rangle]\!], \quad [\![\bar{\sigma}_1]\!] = [\![\langle \sigma_1^0 \rangle]\!] + \varepsilon [\![\langle \sigma_1^1 \rangle]\!]. \tag{41}
$$

Then, we deduce from (33), (39) and (40) the following:

$$
[\![\bar{u}]\!] = \varepsilon \mathcal{B} \left\langle \sigma_1^0 \right\rangle (0, x_2), \quad [\![\bar{\sigma}_1]\!] = -\varepsilon \mathcal{C} \frac{\partial^2 u^0}{\partial x_2^2}(0, x_2). \tag{42}
$$

A.4. The final homogenized problem

The equations in the substrate (26) and the associated jump conditions (33) could be used to solve the homogenized problem iteratively: first compute $\left(u^0, \langle \sigma^0 \rangle\right)$ (compute also $\mathcal{B}$ and $\mathcal{C}$) and use the results to get the right hand-side term in (42); then, compute $\left(u^1, \sigma^1\right)$; finally, we obtain $(\bar{u}, \bar{\sigma})$ in (25) which approximate $(u^\varepsilon, \sigma^\varepsilon)$ up to $O\left(\varepsilon^2\right)$. As discussed in [19], it is preferable to handle a unique problem, and this is done by defining the fields (u^h, σ^h) satisfying the following homogenized problem:

$$\begin{cases} \operatorname{div}\sigma^h + \langle b^*\rangle u^h = 0, \quad \sigma^h = \begin{pmatrix} \langle a^*\rangle & 0 \\ 0 & \langle 1/a^*\rangle^{-1} \end{pmatrix} \nabla u^h, & x_1 < 0, \\ \operatorname{div}\sigma^h + \left(\dfrac{K^*}{K_R}\right)^2 u^h = 0, \quad \sigma^h = \nabla u^h, & x_1 > 0, \\ [\![u^h]\!] = \dfrac{\varepsilon\mathcal{B}}{2}\left[\sigma_1^h(0^-, x_2) + \sigma_1^h(0^+, x_2)\right], \\ [\![\sigma_1^h]\!] = -\dfrac{\varepsilon\,\mathcal{C}}{2}\left[\dfrac{\partial^2 u^h}{\partial x_2^2}(0^-, x_2) + \dfrac{\partial^2 u^h}{\partial x_2^2}(0^+, x_2)\right]. \end{cases} \tag{43}$$

Appendix B. Effective problem in the region of the free stratified edge

To determine the effective problem of (4), we will follow the same idea in [10]. We use the same expansions (19), such that the outer region is for $x_1 > 0$ and an inner region is set in $\mathbf{y} \in \mathbb{R} \times Y$ (with $Y = (-1/2, 1/2)$), where $\tilde{a^*}(\mathbf{y}) = a^*(y_2)$ and $\tilde{b^*}(\mathbf{y}) = b^*(y_2)$, and we define $\mathbf{Y} = (0, +y_1^m) \times Y$. Next, the radiation condition applies in the outer region and the Neumann boundary condition applies for the inner problem only, leading to

$$\tau_1^n(x_2, 0^+, y_2) = 0, \quad n = 0, 1, \ldots. \tag{44}$$

Finally, the continuity of $(u^n, \tau^n \cdot \mathbf{n})$ apply between the layers in the inner and outer problems. The missing conditions for the outer terms when $x_1 \to 0^+$ and for the inner terms when $y_1 \to +\infty$ are provided by the matching conditions (23b)–(23d) and (24b)–(24d).

B.1. Effective boundary conditions

The leading order of (4) tells us that $\operatorname{div}_{\mathbf{y}} \tau^0 = 0$, and integrating over Y with $y_1^m \to +\infty$, leads to

$$\int_Y \mathrm{d}y_2\, \tau_1^0(x_2, +\infty, y_2) = \int_Y \mathrm{d}y_2\, \tau_1^0(x_2, 0^+, y_2) = 0$$

using the continuity of $\tau^0 \cdot \mathbf{n}$ and (44). Thus, using the matching conditions (23d) leads to

$$\left\langle \sigma_1^0 \right\rangle (0^+, x_2) = 0.$$

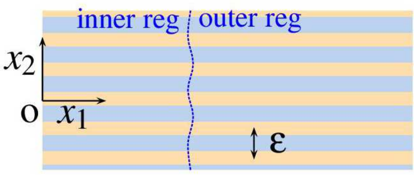

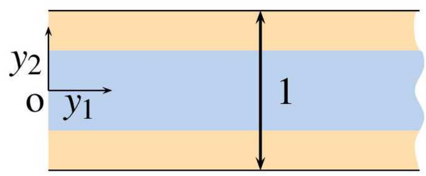

Fig. 14. Left: configuration in the x coordinate; the periodicity along x_2 is $\varepsilon \equiv K_R h$; the inner region corresponds to the neighborhood of the boundary between the stratified medium ($x_1 > 0$) and the surrounding homogeneous medium ($x_1 < 0$). Right: the unit cell (inner region) in the y coordinate, with $\mathbf{y} = \mathbf{x}/\varepsilon$, and $\mathbf{y} \in (-\infty, 0) \times Y$, with $Y = (-1/2, 1/2)$.

Now, we inspect the next order to determine $\langle\sigma_1^1\rangle(0^+, x_2)$, and to do so, we shall define an elementary problem (Figure 14). The same approach as for the jump condition is used, but significant simplifications occur due (i) the cancellation of $\langle\sigma_1^0\rangle(0^+, x_2)$ and (ii) the fact that $\tilde{a^*}(\mathbf{y}) = a^*(y_2)$ in Y. The system (14) now reads

$$\begin{cases} \operatorname{div}_{\mathbf{y}} \boldsymbol{\tau}^0 = 0, \quad \text{with} \quad \tau^0 = a^*(y_2) \left[\dfrac{\partial u^0}{\partial x_2}(0^+, x_2)\mathbf{e}_2 + \boldsymbol{\nabla}_{\mathbf{y}} v^{\mathbf{1}}(x_2, \mathbf{y}) \right], \\ v^1 \ \text{ and } \ \tau^0 \cdot \mathbf{n} \ \text{ continuous at each interface}, \\ \lim\limits_{y_1 \to +\infty} \nabla_{\mathbf{y}} v^1(x_2, \mathbf{y}) = \dfrac{1/a^*(y_2) - \langle 1/a^* \rangle}{\langle 1/a^* \rangle} \dfrac{\partial u^0}{\partial x_2}(0^+, x_2)\mathbf{e}_2, \\ \tau_1^0(x_2, 0^+, y_2) = 0, \end{cases} \tag{45}$$

with v^1 and τ^0 periodic w.r.t y_2. The above system is linear w.r.t $\partial_{x_2} u^0(0^+, x_2)$ and we define $V^{(2)}$ such that

$$v^1(x_2, \mathbf{y}) = \frac{\partial u^0}{\partial x_2}(0^-, x_2) \left[A^*(y_2) + V^{(2)}(\mathbf{y}) \right] + \hat{v}(x_2),$$

with $A^*(y_2)$ defined in (35). As previously, $\hat{v}(x_2)$ has been introduced since v^1 in (45) is defined up to a function of x_2 and as previously, its determination will not be needed. Next, if $V^{(2)}$ satisfies the elementary problem

$$\begin{cases} \operatorname{div} \left[a^*(y_2) \nabla V^{(2)}(\mathbf{y}) \right] = 0, \\ V^{(2)} \ \text{ and } \ a^*(y_2) \nabla V^{(2)}(\mathbf{y}) \cdot \mathbf{n} \ \text{ continuous, } V^{(2)} \text{ periodic w.r.t. } y_2, \\ \lim\limits_{y_1 \to +\infty} \nabla V^{(2)}(\mathbf{y}) = \mathbf{0}, \\ \dfrac{\partial V^{(2)}}{\partial y_1}(0^+, y_2) = 0, \end{cases} \tag{46}$$

then v^1 satisfies (45). The significant simplification is that the above system has an obvious solution $V^{(2)} = \text{const}$. Thus $\tau^0 = \partial_{x_2} u^0(0^+, x_2) \left[\langle 1/a \rangle^{-1} \mathbf{e}_2 + a^*(y_2) \nabla V^{(2)} \right]$, from (45), simplifies in

$$\boldsymbol{\tau}^0(x_2, \mathbf{y}) = \langle 1/a \rangle^{-1} \frac{\partial u^0}{\partial x_2}(0^+, x_2)\mathbf{e}_2.$$

Integrating (4) over $\mathbf{Y}$ at order ε^0, leads to

$$\int_Y d\mathbf{y} \left[\operatorname{div}_{\mathbf{y}} \tau^1(x_2, \mathbf{y}) + \frac{\partial \tau_2^0}{\partial x_2}(x_2, \mathbf{y}) + \tilde{b}(\mathbf{y}) u^0(0, x_2) \right] = 0, \tag{47}$$

and using (44), with

$$\begin{cases} \displaystyle\int_Y d\mathbf{y} \operatorname{div}_{\mathbf{y}} \tau^1(x_2, \mathbf{y}) = \left\langle \tau_1^1 \right\rangle (x_2, 0^+) - \left\langle \tau_1^1 \right\rangle (x_2, +y_1^m) = - \left\langle \tau_1^1 \right\rangle (x_2, +y_1^m), \\ \displaystyle\int_Y d\mathbf{y} \frac{\partial \tau_2^0}{\partial x_2}(x_2, \mathbf{y}) = y_1^m \langle 1/a \rangle^{-1} \frac{\partial^2 u^0}{\partial x_2^2}(0^+, x_2), \\ \displaystyle\int_Y d\mathbf{y}\, \tilde{b}(\mathbf{y}) u^0(0^+, x_2) = y_1^m \langle b \rangle u^0(0^+, x_2). \end{cases}$$

Summing up three terms above as in (47) and using the system at $x_1 = 0^+$, which is obtained from (28) for $x_1 < 0$ and (26) for $x_1 > 0$

$$\begin{cases} -\dfrac{\partial \left\langle \sigma_1^0 \right\rangle}{\partial x_1}(0^-, x_2) = \langle 1/a \rangle^{-1} \dfrac{\partial^2 u^0}{\partial x_2^2}(0, x_2) + \langle b \rangle u^0(0, x_2), \\ -\dfrac{\partial \left\langle \sigma_1^0 \right\rangle}{\partial x_1}(0^+, x_2) = \dfrac{\partial^2 u^0}{\partial x_2^2}(0, x_2) + u^0(0, x_2), \end{cases}$$

we get

$$\left\langle \tau_1^1 \right\rangle (x_2, +y_1^m) + y_1^m \frac{\partial \left\langle \sigma_1^0 \right\rangle}{\partial x_1}(0^+, x_2) = 0,$$

and from the matching condition (24c)–(24d) at $x_1 = 0^+$, we get

$$\left\langle \sigma_1^1 \right\rangle (0^+, x_2) = 0.$$

It follows that up to order 2, the boundary condition on a rigid wall remains of the Neumann type, and for $\bar{\sigma}(\mathbf{x})$ defined in (25), we get

$$\overline{\sigma}_1(0^+, x_2) = 0.$$

B.2. The final homogenized problem

Following the same procedure as in subsection A.4, we get the effective problem in the region of free stratified edge, which reads

$$\begin{cases} \operatorname{div} \boldsymbol{\sigma}^h + \langle b^* \rangle u^h = 0, \quad \boldsymbol{\sigma}^h = \begin{pmatrix} \langle a^* \rangle & 0 \\ 0 & \langle 1/a^* \rangle^{-1} \end{pmatrix} \nabla u^h, \quad x_1 > 0, \\ {\sigma_1}^h (0^+, x_2) = 0. \end{cases}$$

[1] Cioranescu D., Donato P. An Introduction to Homogenization. No. 17 in Oxford Lecture Series in Mathematics and Its Applications. Oxford, New York, Oxford University Press (1999).

[2] Li Q., Chen W., Liu S., Wang J. A novel implementation of asymptotic homogenization for viscoelastic composites with periodic microstructures. Composite Structures. **208**, 276–286 (2019).

[3] Marigo J.-J., Maurel A. Homogenization models for thin rigid structured surfaces and films. The Journal of the Acoustical Society of America. **140** (1), 260–273 (2016).

[4] Marigo J.-J., Pideri C. The Effective Behavior of Elastic Bodies Containing Microcracks or Microholes Localized on a Surface. International Journal of Damage Mechanics. **20** (8), 1151–1177 (2011).

[5] Marigo J.-J., Maurel A, Pham K., Sbitti A. Effective Dynamic Properties of a Row of Elastic Inclusions: The Case of Scalar Shear Waves. Journal of Elasticity. **128** (2), 265–289 (2017).

[6] Delourme B. High-order asymptotics for the electromagnetic scattering by thin periodic layers. Mathematical Methods in the Applied Sciences. **38** (5), 811–833 (2015).

[7] Delourme B., Haddar H., Joly P. Approximate Models for Wave Propagation across Thin Periodic Interfaces. Journal de Mathématiques Pures et Appliquées. **98** (1), 28–71 (2012).

[8] Bonnet–Bendhia A. S., Drissi D., Gmati N. Simulation of Muffler's Transmission Losses by a Homogenized Finite Element Method. Journal of Computational Acoustics. **12** (03), 447–474 (2004).

[9] Marigo J.-J., Maurel A. Second Order Homogenization of Subwavelength Stratified Media Including Finite Size Effect. SIAM Journal on Applied Mathematics. **77** (2), 721–743 (2017).

[10] Marigo J.-J., Maurel A. Supplementary Materials: Second Order Homogenization of Subwavelength Stratified Media Including Finite Size Effect. **13** (2017).

[11] Borcherdt R. D. Viscoelastic Waves in Layered Media. Cambridge, Cambridge University Press (2009).

[12] Maurel A., Pham K. Multimodal method for the scattering by an array of plates connected to an elastic half-space. The Journal of the Acoustical Society of America. **146** (6), 4402–4412 (2019).

[13] Gumerov N. A., Duraiswami R. Fast Multipole Methods for the Helmholtz Equation in Three Dimensions. Elsevier Series in Electromagnetism. 171–223 (2004).

[14] Marigo J.-J., Maurel A. An Interface Model for Homogenization of Acoustic Metafilms. World Scientific Handbook of Metamaterials and Plasmonics. 599–645 (2017).

[15] Petit R. A Tutorial Introduction. In: Petit R. (eds) Electromagnetic Theory of Gratings. Topics in Current Physics, vol. 22. Springer, Berlin, Heidelberg (1980). Petit R, (auth.), Petit P. R. (eds.).

[16] Maurel A., Félix S., Mercier J.-F., Ourir A. Effective birefringence to analyze sound transmission through a layer with subwavelength slits. Comptes Rendus Mécanique. **343** (12), 612–621 (2015).

[17] Lalanne P., Lemercier-Lalanne D. Depth dependence of the effective properties of subwavelength gratings. Journal of the Optical Society of America A. **14** (2), 450–459 (1997).

[18] Abdelmoula R., Marigo J.-J. The effective behavior of a fiber bridged crack. Journal of the Mechanics and Physics of Solids. **48** (11), 2419–2444 (2000).

[19] David M., Marigo J.-J., Pideri C. Homogenized Interface Model Describing Inhomogeneities Located on a Surface. Journal of Elasticity. **109** (2), 153–187 (2012).

Гомогенізація субхвильового вільного стратифікованого краю в'язкопружного середовища з врахуванням скінченно-розмірного ефекту

Белемоу Р.[1], Сбітті А.[2], Маріго Ж.-Ж.[3], Цулі А.[4]

[1] *Університет Хасана II, Енс,*
вул. Ель Джадіда Км 9, Ганді, 50069, Касабланка, Марокко
[2] *Університет Мохаммеда V, Енсам,*
вул. Об'еднаних Націй, Агдал, 8007.N.U, Рабат, Марокко
[3] *Лабораторія механіки твердого тіла, Політехнічна школа,*
91128, Палезо, Франція
[4] *Університет Хасана II, Енсам,*
вул. Ніла, 150, Сіді Отман, 20670, Касабланка, Марокко

У цій статті пропонується гомогенізація стратифікованого в'язкопружного середовища з вільним краєм. Розглядається вплив двовимірної періодично стратифікованої плити на напівнескінченним в'язкопружним ґрунтом на поширення зсувних хвиль, що падають на поверхню розділу. У межах гармонічного режиму для отримання еквівалентної анізотропної плити, пов'язаної з ефективними граничними умовами та умовами стрибка для зміщення та нормального напруження на межі поділу, використовується метод гомогенізації другого порядку та узгоджених асимптотичних розвинень. Коефіцієнти відбиття та поля переміщень отримані в замкнених формах, і їх достовірність перевіряється шляхом порівняння з прямими числами у випадку шарів, які пов'язані з граничними умовами Неймана.

Ключові слова: *гомогенізація; узгоджене асимптотичне розвинення; відбиття хвиль; в'язкопружне; стратифіковане середовище; умови ефективного стрибка.*